Vibrational Spectra and Dynamics of Electronically Excited Semiconducting Single-Walled Carbon Nanotubes†

Ying-Zhong Ma, Matthew W. Graham, Matthew A. Prantil, Aaron J. Van Tassle, and Graham R. Fleming*

Department of Chemistry, University of California, Berkeley, and Physical Biosciences Division, Lawrence Berkeley National Laboratory, Berkeley, California 94720-1460

Received: June 30, 2008; Revised Manuscript Received: July 25, 2008

Femtosecond mid-infrared spectroscopy was applied to study the vibrational spectra and dynamics in the electronic excited states of semiconducting single-walled carbon nanotubes (SWNTs). The experiments were performed by exciting SWNTs dispersed individually in polymethylmethacrylate and polyvinyl alcohol polymer films with 40 fs laser pulses at 800 nm, and the resulting responses were monitored with broadband mid-infrared pulses ranging from 1510 to 1670 cm^{-1}. The structured spectra observed show vibrational bands with up-shifted frequencies by $\sim$10−50 cm^{-1} with respect to their ground-state counterparts. The observation provides direct evidence for the theoretically predicted lattice distortions in the electronic excited state. Analysis of the kinetics probed in the mid- and near-infrared regions provide an estimate of the time scales for the vibrational relaxation.

Introduction

The remarkable electronic properties of single-walled carbon nanotubes (SWNT) have stimulated enormous interest in studying their fundamental physics using both frequency- and time-domain spectroscopic methods (for an overview, see recent reviews[1−5]). Over the past few years, application of ultrafast spectroscopy has revealed important information on fundamental dynamics, such as electron−phonon scattering, exciton−exciton annihilation, intrinsic relaxation, and some extrinsic effects (see the review by Ma et al.[4] and the references therein). However, all these studies have been primarily focused on electronic excited states.

It has been predicted theoretically that creation of an exciton in a semiconducting SWNT leads to a long-ranged distortion in its lattice.[6−8] The resulting change in the bond length in the electronically excited SWNT can lead to different vibrational frequencies from the corresponding ground state. The transition from this distorted lattice to a new equilibrium lattice geometry, or vibrational relaxation, in the electronically excited state can further have profound effects on the relaxation of the electronic excited state itself. This suggests that vibrational relaxation in the electronically excited states is an integral part of the overall dynamical process. In this paper, we report a femtosecond mid-IR spectroscopic study on the vibrational spectra and dynamics of electronically excited semiconducting SWNTs.

Experimental Section

The experiments were performed on $\sim$100 μm thick films of SWNTs fabricated using either polymethylmethacrylate (PMMA)[9] or polyvinyl alcohol (PVA) as the embedding matrix. Both polymers have good transmission in the mid-IR region necessary for the transient absorption (TA) measurements. Our starting material was a commercial H_2O suspension of CoMoCAT SWNTs (SouthWest Nano Tech.), which were dispersed individually with sodium dodecylbenzene sulfonate (NaDDBS) as a surfactant. The linear absorption spectra of these films and the starting aqueous solution are shown in Figure 1. Although the spectra of the films exhibit a noticeable shift and a background change with respect to the solution spectrum, the main features associated with both the lowest and the second dominant exciton transitions (E_{11} and E_{22}) of the two most abundant tube types, the (6, 5) and (7, 5) tubes, are unchanged. This excludes the occurrence of any significant tube aggregation, which would have substantially washed out these distinct features.[10] This conclusion is further supported by the observed steady-state fluorescence emission spectra with a clearly weaker emission around 1150 nm than from those dominant tube species (data not shown).[11,12] Measurement of the fluorescence emission and excitation spectra further enabled us to determine the E_{11} (and E_{22}) transition wavelengths for both the (6, 5) and (7, 5) nanotubes.[13] For the SWNT/PMMA film, we found 1004 and 1034 (572 and 647) nm, respectively. Blank PMMA and PVA

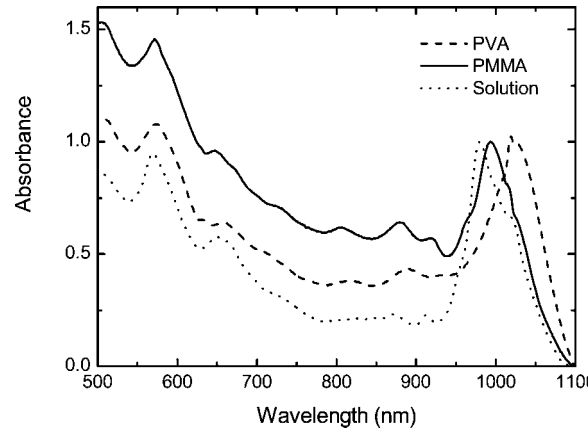

Figure 1. Linear absorption spectra of the aqueous suspension of CoMoCAT nanotubes (dotted line) and the nanotube films, which were prepared using this solution and PVA (dashed line) and PMMA (solid line) polymers.

† Part of the Karl Freed Festschrift.

* To whom correspondence should be addressed. E-mail: GRFleming@lbl.gov.

10.1021/jp805745k CCC: $40.75
Published on Web 09/25/2008

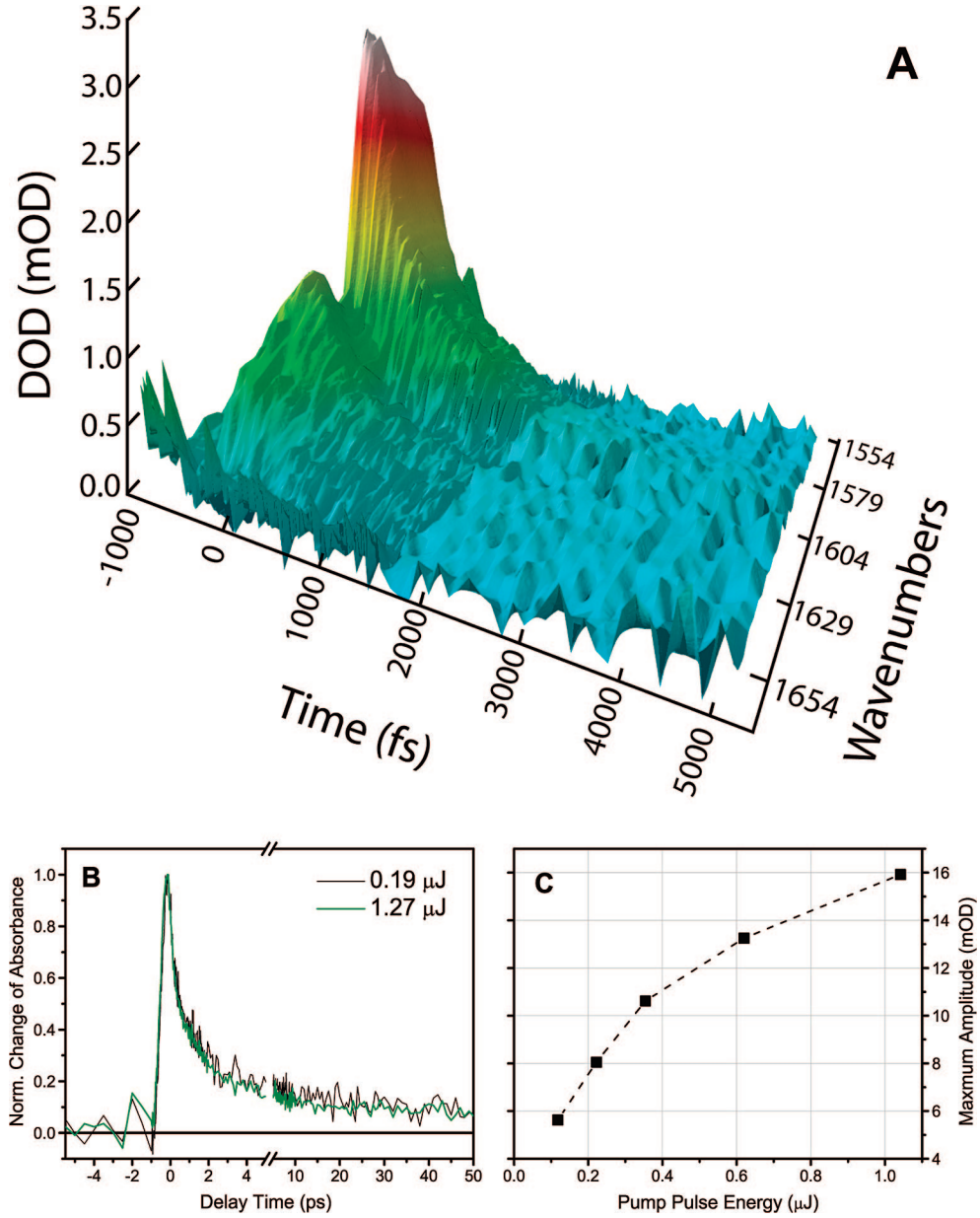

Figure 2. (a) Representative TA spectrum from 1554 to 1654 cm^{-1}, recorded using the SWNT/PMMA film at a pump intensity of 2.5 mJ/cm^2 at 800 nm. (b) The normalized ΔOD kinetic profiles obtained at 1603 cm^{-1} under two different pump intensities: 0.61 mJ/cm^2 (black line) and 4.1 mJ/cm^2 (dark green line). (c) Plot of the maximum magnitude of the TA signal at 1603 cm^{-1} as a function of pump intensity.

films with NaDDBS surfactant were also prepared in order to experimentally quantify their potential contributions to the TA signals in the spectral region of interest.

We employed a light source that consists of a 1 kHz Ti:sapphire regenerative amplifier and a mid-IR optical parametric amplifier (OPA). The former produces 800 nm pulses with typical duration of 40 fs (full-width at half-maximum, fwhm), whereas the latter generates short pulses tunable between 3 and 7 μm (3300−1400 cm^{-1}) with a duration of 95 fs (fwhm) at 5 μm and a pulse energy of 1−2 μJ. The 800 nm pulses were used as the pump beam, and induced changes of sample absorbance were monitored with broadband mid-IR pulses. The detection system involves a Triax 180 imaging spectrometer with 4 cm^{-1} resolution and a 64-element HgCdTe dual-array detector attached to an IR64-16 multichannel laser pulse integrator system. The pump beam was focused to a spot of ~200 μm on the sample, and its polarization was set parallel to the probe beam. For a detailed description of the light source and the experimental setup, see ref 14. The near-IR TA data were collected using a setup that consists of a 250 kHz Ti:sapphire regenerative amplifier and a visible OPA. We refer to our previous papers for the experimental details.[15,16]

Results and Discussion

We found that a pump pulse intensity ranging from 0.64 to 3.2 mJ/cm^2 was necessary to acquire data with a satisfactory signal-to-noise ratio. Representative TA spectra recorded at a pump intensity of 2.5 mJ/cm^2 using the SWNT/PMMA film are shown in Figure 2a. The TA spectra show positive-signed, induced absorption in the entire probe spectral region (1510−1670 cm^{-1}) with several distinct features. Besides the broad band peaking around 1600 cm^{-1}, distinct sidebands with peaks located at 1563 and 1633 cm^{-1} are prominent. Comparison of the TA spectra measured at five other pump intensities (0.38, 0.70, 1.12, 1.98, and 3.33 mJ/cm^2) shows that, upon normalizing at the

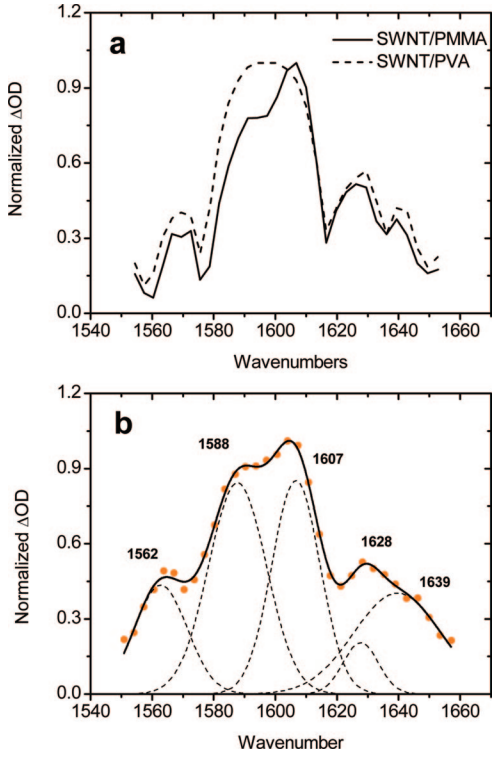

Figure 3. (a) Comparison of the TA spectra measured using the SWNT/PMMA (solid line) and SWNT/PVA (dashed line) films at a delay time of 100 fs. For ease of comparison, these spectra are scaled to equal amplitude at their maxima. (b) TA spectrum recorded for the SWNT/PMMA film at a delay time of 100 fs (symbols). The Gaussian components resulting from spectral deconvolution are shown as dashed lines, and the fit spectrum is given by the solid line. The positions of the peaks are labeled on the figure.

maxima of the main bands peaking around 1600 cm^{-1}, the spectral shape observed at any given delay time is independent of intensity. This invariance consequently leads to dynamics that are independent of pump intensity at all probe frequencies. As an example, Figure 2b shows the normalized kinetic profiles obtained at 1603 cm^{-1} under two different pump intensities. Fitting the kinetics by employing a sum of exponential terms as a model function and by taking into account the finite duration of the pump and probe pulses gives the following timescales (relative amplitudes): 0.21 ps (0.63), 1.66 ps (0.30), and 81 ps (0.07). Note that 81 ps is a rough estimate for the time scale of a long-lived decay component that persists over the entire range of our scan (700 ps). The maximum magnitude of the TA signal is further found to increase with pump intensity in a nonlinear, saturating manner (Figure 2c). The independence of the kinetic decay on pump intensity (Figure 2b) and the saturating behavior of its signal magnitude with increasing intensity (Figure 2c) are qualitatively similar to what has been found in the near-IR region where the E_{11} transition of selected semiconducting SWNTs is probed following its direct optical excitation.[15]

Although the PMMA and PVA polymers as well as the NaDDBS surfactant absorb in the spectral region of our measurements, none of them should contribute to the observed TA signals. The reason is that they are not excited by the 800 nm pump pulse and the finite absorption of the mid-IR probe pulse is already subtracted off in the obtained TA data. This is confirmed by our test measurements performed at a pump intensity of 3.68 mJ/cm^2 on a reference PMMA film containing just the surfactant. The result shows weak transients around time zero with either positive- or negative-signed signals depending on the probe frequency, arising most likely from a pulse overlapping effect (data not shown). Also, the maximum magnitude of the detected signal is less than 1.5% of the signal maximum observed from the SWNT/PMMA film at a similar pump intensity (3.33 mJ/cm^2). We therefore neglect this weak signal in the rest of the paper. We further found that use of the PVA polymer does not cause any significant changes in both TA spectra and kinetics (as an example, see Figure 3b, c), suggesting that the results obtained are intrinsic to nanotubes. Furthermore, both the spectral and kinetic features are found to be independent of sample position for the SWNT/PMMA and SWNT/PVA films, even though the magnitudes of the TA signals can vary considerably from one location to another.

TABLE 1: Summary of the Vibrational Frequencies Determined in This Work and by Raman and Infrared Experiments[a]

frequency (cm^{-1})	state	method	material	reference
1562	E_{11}	TA	individualized tubes	this work
1588	E_{11}	TA	individualized tubes	this work
1607	E_{11}	TA	individualized tubes	this work
1628	E_{11}	TA	individualized tubes	this work
1640	E_{11}	TA	individualized tubes	this work
1554	GS	Raman	isolated tubes	27
1563	GS	Raman	isolated tubes	27
1571	GS	Raman	isolated tubes	27
1591	GS	Raman	isolated tubes	27
1600	GS	Raman	isolated tubes	27
1541	GS	IR	purified bundles	24
1564	GS	IR	purified bundles	24
1585	GS	IR	purified bundles	24
1587	GS	IR	bundles	25

[a] GS stands for ground state.

The positive-signed TA signals observed indicate that they must originate from electronic excited state(s). A transition from such excited state(s) in the frequency region of our measurements, in principle, can be either electronic or vibrational depending solely on the nature of the final state(s). From an energetic point of view, an electronic, intraband excitonic transition appears plausible because of the presence of an exciton-manifold above the E_{11} state.[17] However, the line-widths observed in the TA spectra are too narrow for such an intraband excitonic transition. Because of the short lifetime associated with an excitonic state lying above the E_{11} state, its involvement in the intraband transition should result in a much broader spectrum than we observe. The well-studied E_{22} state can serve as a typical example here: its lifetime was determined to be in the order of 50 fs for several semiconducting tube species.[18,19] This short lifetime gives rise to a broad spectrum with a typical fwhm of 350 cm^{-1} or more.[20,21] This is in stark contrast to the narrow line-widths of the observed TA spectra. Analysis of the TA spectrum measured at a delay time of 100 fs shows that the spectrum can be decomposed into five Gaussian components with peaks (fwhm widths) at 1562 (20.1), 1588 (22.2), 1607 (18.5), 1628 (13.5), and 1640 (33.3) cm^{-1}, respectively (see Figure 3b). The fwhm widths of the two major components peaking at 1588 and 1607 cm^{-1} are almost identical to the width of the G-band Raman spectrum measured using the same nanotube material in solution and embedded in polyvinylpyrrolidone (PVP) polymer (data not shown). On the basis of these considerations, we attribute the observed TA spectra to the transition between the levels of the tangential vibrations in the E_{11} excited state(s).

Among the five spectral components shown in Figure 3b for the E_{11} excited-state vibrations, three are characterized by a

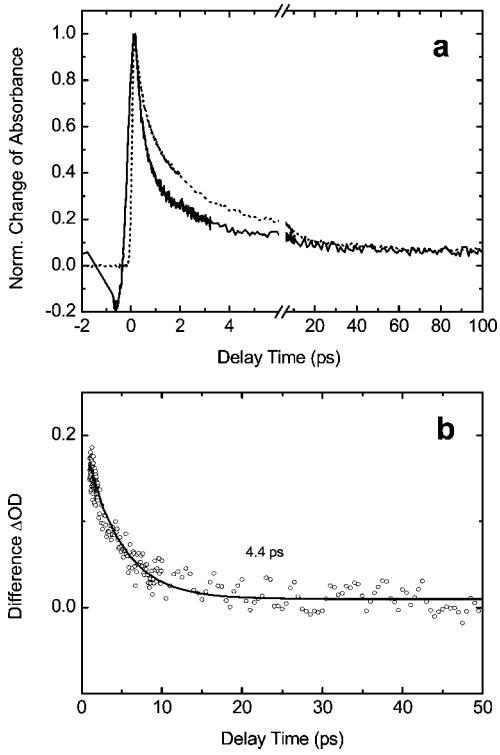

Figure 4. (a) Comparison of the TA kinetics detected at 1603 cm^{-1} (800 nm pump) (solid lines) and at 1018 nm (572 nm pump) (dashed lines) for the SWNT/PMMA film. For ease of comparison, the data collected at 1018 nm are inverted by multiplying (−1). The kinetic traces are normalized at the signal maxima. (b) The difference between the two kinetic profiles shown in (a) and its monoexponential decay fit (solid line).

frequency that is up-shifted by ∼10−50 cm^{-1} with respect to the frequencies of the electronic ground-state vibrations. Electronic ground-state vibrations have been a subject of extensive studies by resonant Raman spectroscopy at both single-tube and ensemble levels (see the review by Dresselhaus et al.[22]). Fewer investigations based on theoretical[23] and experimental[24,25] infrared spectroscopy have been also reported. In Table 1, we summarize the vibrational frequencies determined in this work (for the excited state) together with the ground-state frequencies reported in the literature from Raman and infrared measurements. Although some variations exist in the results reported for the tangential vibrations, the frequencies found from a majority of work are below 1600 cm^{-1}. The clearly up-shifted frequencies observed in this work provide a direct evidence for the occurrence of a long-ranged lattice distortion in the electronic excited state.[6−8] We further speculate that the appearance of multiple spectral components as shown in Figure 3b may be indicative of a bond-length alternation in the distorted lattice. In the recent calculations of Tretiak and coworkers,[7] a corrugated tube surface arising from alternative lengthening and shortening of bond lengths was predicted for a semiconducting SWNT. Note that such a bond-length alternation may give rise to both down- and up-shifted vibrational frequencies compared to the ground state.

Analysis of the temporal evolution of the TA kinetics probed in the mid- and near-IR regions enables us to estimate the time scale of the vibrational relaxation in the E_{11} state. Because the evolution of the mid-IR kinetics is governed by the relaxation from both the final vibrational state and the E_{11} electronic state, the contribution from the electronic relaxation must be removed. For this purpose, we performed separate experiments in the near-IR region to characterize the exciton population relaxation from the E_{11} state and the concomitant recovery of the ground state. The dashed-line curve in Figure 4 shows the data obtained from the same SWNT/PMMA film at 1018 nm, the E_{11} state of the (6, 5) tube, which is one of the dominant nanotube species in the sample. Selective detection of this particular tube type is accomplished by resonant excitation of its E_{22} state at 572 nm. As is evident from Figure 4a, the kinetic profile probed at 1603 cm^{-1} exhibits a faster decay than the one measured at 1018 nm. The difference between these two kinetic profiles represents approximately the dynamics of the vibrational relaxation in the E_{11} state. As shown in Figure 4b, this difference kinetics can be well described by a single time scale of 4.4 ps. A similar value was also obtained for the data measured using the SWNT/PVA film. Note that this time scale should be considered as a rough estimate as the mid- and near-IR data were measured under electronically nonresonant and resonant conditions, respectively.

As a final remark, we briefly discuss the work of Zhao et al.[26] that covers a similar spectral range. The authors reported a TA spectrum measured on a film sample prepared by dispersing the HiPco tubes into a PVA matrix. The published spectrum is very different from ours in terms of the overall shape, due to the use of different tube materials (HiPco vs CoMoCAT) and different spectral resolution (4 cm^{-1} in our case and roughly 160 cm^{-1} in the case of ref 26). The authors attributed this band to intraband excitonic transitions from both the lowest optically allowed and dark excitonic states to some higher-lying ones.

In summary, we demonstrated in this report that femtosecond TA spectroscopy employing 800 nm pump and mid-IR probe enables access to the vibrational spectra and dynamics in the E_{11} exciton states of semiconducting SWNTs. The observed induced absorption spectra exhibit prominent spectral structures, which can be decomposed into five Gaussian components. Three of these components are characterized by a frequency up-shifted by ∼10−50 cm^{-1} with respect to the frequencies of the electronic ground-state vibrations. This observation provides a direct evidence for the occurrence of a long-ranged lattice distortion in the electronic excited state. Analysis of the TA kinetics probed in the mid- and near-IR regions enables us to extract an approximate time scale for the vibrational relaxation. Further studies employing single tube enriched samples in combination with resonant excitation are expected to provide a more accurate determination of the time scales.

Acknowledgment. This work was supported by the NSF. Portions of this work were performed at the Molecular Foundry, Lawrence Berkeley National Laboratory, which is supported by the Office of Science, Office of Basic Energy Sciences, of the U.S. Department of Energy under Contract No. DE-AC02−05CH11231.

References and Notes

(1) Hartschuh, A. New techniques for carbon-nanotube study and characterization. In *Topics in Applied Physics*; Jorio, A., Dresselhaus, G., Dresselhaus, M. S., Eds.; Springer-Verlag Berlin: Heidelberg, Germany, 2008; Vol. 111, p 371.

(2) Heinz, T. F. Rayleigh scattering spectroscopy. In *Topics in Applied Physics*; Jorio, A., Dresselhaus, G., Dresselhaus, M. S., Eds.; Springer-Verlag Berlin: Heidelberg, Germany, 2008; Vol. 111, p 353.

(3) Lefebvre, J.; Maruyama, S.; Finnie, P. Photoluminescence: science and applications. In *Topics in Applied Physics*; Jorio, A., Dresselhaus, G., Dresselhaus, M. S., Eds.; Springer-Verlag Berlin: Heidelberg, Germany, 2008; Vol. 111, p 287.

(4) Ma, Y.-Z.; Hertel, T.; Vardeny, Z. V.; Fleming, G. R.; Valkunas, L. Ultrafast spectroscopy of carbon nanotubes. In *Topics in Applied Physics*; Jorio, A., Dresselhaus, G., Dresselhaus, M. S., Eds.; Springer-Verlag Berlin: Heidelberg, Germany, 2008; Vol. 111, p 321.

(5) Saito, R.; Fantini, C.; Jiang, J. Excitonic states and resonance Raman spectroscopy of single-wall carbon nanotubes. In *Topics in Applied Physics*; Jorio, A., Dresselhaus, G., Dresselhaus, M. S., Eds.; Springer-Verlag Berlin: Heidelberg, Germany, 2008; Vol. 111, p 251.

(6) Perebeinos, V.; Avouris, P. *Phys. Rev. Lett.* **2005**, *94*, 027402.

(7) Tretiak, S.; Kilina, S.; Piryatinski, A.; Saxena, A.; Martin, R. L.; Bishop, A. R. *Nano Lett.* **2007**, *7*, 86.

(8) Kilina, S.; Tretiak, S. *Adv. Func. Mater.* **2007**, *17*, 3405.

(9) Ma, Y.-Z.; Valkunas, L.; Bachilo, S. M.; Fleming, G. R. *Phys. Chem. Chem. Phys.* **2006**, *8*, 5689.

(10) O'Connell, M. J.; Bachilo, S. M.; Huffman, C. B.; Moore, V. C.; Strano, M. S.; Haroz, E. H.; Rialon, K. L.; Boul, P. J.; Noon, W. H.; Kittrell, C.; Ma, J.; Hauge, R. H.; Weisman, R. B.; Smalley, R. E. *Science* **2002**, *297*, 593.

(11) Torrens, O. N.; Milkie, D. E.; Zheng, M.; Kikkawa, J. M. *Nano Lett.* **2006**, *6*, 2864.

(12) Tan, P. H.; Rozhin, A. G.; Hasan, T.; Hu, P.; Scardaci, V.; Milne, W. I.; Ferrari, A. C. *Phys. Rev. Lett.* **2007**, *99*, 137402.

(13) Bachilo, S. M.; Balzano, L.; Herrera, J. E.; Pompeo, F.; Resasco, D. E.; Weisman, R. B. *J. Am. Chem. Soc.* **2003**, *125*, 11186.

(14) van Tassle, A. J.; Prantil, M. A.; Fleming, G. R. *J. Phys. Chem. B* **2006**, *110*, 18989.

(15) Ma, Y.-Z.; Valkunas, L.; Dexheimer, S. L.; Bachilo, S. M.; Fleming, G. R. *Phys. Rev. Lett.* **2005**, *94*, 157402.

(16) Ma, Y.-Z.; Valkunas, L.; Dexheimer, S. L.; Fleming, G. R. *Mol. Phys.* **2006**, *104*, 1179.

(17) Ma, Y.-Z.; Spataru, C. D.; Valkunas, L.; Louie, S. G.; Fleming, G. R. *Phys. Rev. B* **2006**, *74*, 085402.

(18) Ma, Y.-Z.; Stenger, J.; Zimmermann, J.; Bachilo, S. M.; Smalley, R. E.; Weisman, R. B.; Fleming, G. R. *J. Chem. Phys.* **2004**, *120*, 3368.

(19) Manzoni, C.; Gambetta, A.; Menna, E.; Meneghetti, M.; Lanzani, G.; Cerullo, G. *Phys. Rev. Lett.* **2005**, *94*, 207401.

(20) Lefebvre, J.; Fraser, J. M.; Finnie, P.; Homma, Y. *Phys. Rev. B* **2004**, *69*, 075403.

(21) Miyauchi, Y.; Maruyama, S. *Phys. Rev. B* **2006**, *74*, 035415.

(22) Dresselhaus, M. S.; Dresselhaus, G.; Saito, R.; Jorio, A. *Phys. Reports* **2005**, *409*, 47.

(23) Sbai, K.; Rahmani, A.; Chadli, H.; Bantignies, J.-L.; Hermet, P.; Sauvajol, J.-L. *J. Phys. Chem. B* **2006**, *110*, 12388.

(24) Kim, U. J.; Liu, X. M.; Furtado, C. A.; Chen, G.; Saito, R.; Jiang, J.; Dresselhaus, M. S.; Eklund, P. C. *Phys. Rev. Lett.* **2005**, *95*, 157402.

(25) Bantignies, J.-L.; Sauvajol, J.-L.; Rahmani, A.; Flahaut, E. *Phys. Rev. B* **2006**, *74*, 195425.

(26) Zhao, H.; Mazumdar, S.; Sheng, C.-X.; Tong, M.; Vardeny, Z. V. *Phys. Rev. B* **2006**, *73*, 075403.

(27) Jorio, A.; Pimenta, M. A.; Souza Filho, A. G.; Samsonidze, G. G.; Swan, A. K.; Ünlü, M. S.; Goldberg, B. B.; Saito, R.; Dresselhaus, G.; Dresselhaus, M. S. *Phys. Rev. Lett.* **2003**, *90*, 107403.

JP805745K